

General Disclaimer

One or more of the Following Statements may affect this Document

- This document has been reproduced from the best copy furnished by the organizational source. It is being released in the interest of making available as much information as possible.
- This document may contain data, which exceeds the sheet parameters. It was furnished in this condition by the organizational source and is the best copy available.
- This document may contain tone-on-tone or color graphs, charts and/or pictures, which have been reproduced in black and white.
- This document is paginated as submitted by the original source.
- Portions of this document are not fully legible due to the historical nature of some of the material. However, it is the best reproduction available from the original submission.



NASA CR-156742

POWER LAW RELATIONSHIPS FOR RAIN ATTENUATION
AND REFLECTIVITY

D. M. J. Devasirvatham
D. B. Hodge

(NASA-CR-156742) POWER LAW RELATIONSHIPS
FOR RAIN ATTENUATION AND REFLECTIVITY (Ohio
State Univ., Columbus.) 19 F HC A02/MF A01
CSSL 20N

N78-22269

G3/32 Unclas
16374

The Ohio State University

ElectroScience Laboratory

Department of Electrical Engineering
Columbus, Ohio 43212

Technical Report 784650-2

January 1978



National Aeronautics and Space Administration
GODDARD SPACE FLIGHT CENTER
Greenbelt, Maryland 20771

TECHNICAL REPORT STANDARD TITLE PAGE

1. Report No.	2. Government Accession No.	3. Recipient's Catalog No.	
4. Title and Subtitle POWER LAW RELATIONSHIPS FOR RAIN ATTENUATION AND REFLECTIVITY		5. Report Date January 1978	6. Performing Organization Code
		8. Performing Organization Report No. ESL 784650-2	
7. Author(s) D.M.J. Devasirvatham and D.B. Hodge		10. Work Unit No.	
9. Performing Organization Name and Address The Ohio State University ElectroScience Laboratory, Department of Electrical Engineering, Columbus, Ohio 43212		11. Contract or Grant No. NAS5-23850	
		13. Type of Report and Period Covered Technical Report	
12. Sponsoring Agency Name and Address NASA, GSFC Greenbelt, Maryland 20771 E. Hirschmann, Code 953, Technical Officer		14. Sponsoring Agency Code	
		15. Supplementary Notes	
16. Abstract <p>The equivalent reflectivity, specific attenuation and volumetric backscatter cross section of rain are calculated and tabulated at a number of frequencies from 1 to 500 GHz using classical Mie theory. The first two parameters are shown to be closely approximated as functions of rain rate by the power law aR^b. The a's and b's are also tabulated and plotted for convenient reference.</p>			
17. Key Words (Selected by Author(s)) Power law Radar Rain attenuation Millimeter wave Reflectivity Microwave Rain scattering		18. Distribution Statement	
19. Security Classif. (of this report) U	20. Security Classif. (of this page) U	21. No. of Pages 18	22. Price*

I. INTRODUCTION

The shift towards ever higher frequencies for communication links and radars has focused attention on the effects of rain in these applications. The presence of liquid water in the form of rain can have deleterious effects in such cases with the major problem being signal attenuation which causes deep fading. Hence, a knowledge of the attenuation to be expected is essential to the design of such systems. Weather radar systems at frequencies of high attenuation possess certain advantages such as high resolution and sensitivity as well as ease of calibration using the saturation effect as reported in Reference [1]. Again, the measurement of rain rate presupposes a knowledge of the reflectivity and attenuation parameters of rain at the frequency of measurement.

Both equivalent reflectivity and specific attenuation can be approximated closely as functions of rain rate by power laws of the form aR^b , where R is the rain rate in mm/hr. Theoretical justification has been developed in the case of specific attenuation [2] and the a and b values have been computed for limited cases by several researchers and summarized in References [2,3]. However, it appears that a consistent tabulation of the a 's and b 's for both equivalent reflectivity and specific attenuation over a broad frequency range does not exist in the readily available literature. Consequently this report is intended to satisfy this need.

The results of calculations of equivalent reflectivity, specific attenuation and volumetric radar backscatter cross section and of the a 's and b 's for specific attenuation and equivalent reflectivity are presented for frequencies from 1 to 500 GHz. Classical Mie theory is used to calculate the radar cross sections of spherical drops; and the Marshall and Palmer negative exponential drop size distribution is assumed. Rain rates from 1.52 to 152.4 mm/hr are used and the temperature of the water drops is taken to be 0°C.

II. CALCULATIONS

The relevant theoretical results of Mie for scattering by dielectric spheres [4] were recast into a form more suitable for computation and are given in the Appendix. These are used to calculate the total attenuation cross section, $Q_t(m^2)$, and the backscatter cross section, $Q_b(m^2)$, as functions of drop diameter D .

The complex refractive index of water, n_c , is an important parameter in the above calculations. It is strongly dependent on frequency and more weakly on temperature. These properties are discussed in Reference [5].

Next the Marshall and Palmer drop size distribution was assumed [6]. It is of the form

$$N(D) = N_0 e^{-\Lambda D} \text{ [drops/m}^3 \cdot \text{mm]} \quad (1)$$

where

$$\begin{aligned} \Lambda &= \alpha R^\beta \\ N_0 &= 8000/\text{m}^3 \cdot \text{mm} \\ \alpha &= 4.1/\text{mm} \\ \beta &= -0.21 \end{aligned}$$

where R is the rain rate in mm/hr and D is in mm. Then the specific attenuation is [7]

$$\alpha_t = 4.343 \times 10^3 \int_0^\infty Q_t N(D) dD \quad \text{dB/km} \quad (2)$$

and the volumetric radar backscatter cross section is

$$\eta = \int_0^\infty Q_b N(D) dD \quad \text{m}^2/\text{m}^3 \quad (3)$$

The equivalent reflectivity may be defined in terms of the volumetric radar backscatter cross section as

$$Z_{\text{eq}} = \frac{10^6 \lambda^4 \eta}{\pi^5 |K|^2} \quad \text{mm}^6/\text{m}^3 \quad (4)$$

$$= 10 \log_{10} \left(\frac{10^6 \lambda^4 \eta}{\pi^5 |K|^2} \right) \quad \text{dBZ} \quad (5)$$

where

$$K = \frac{n_c^2 - 1}{n_c^2 + 2} \quad (6)$$

and λ is the wavelength in mm. This definition is equivalent to that associated with Rayleigh scattering, but remains useful at higher frequencies as well.

The values of α_t and Z_{eq} were calculated at 36 frequencies from 1 to 500 GHz for 7 rain rates of 1.52, 2.54, 12.7, 25.4, 50.8, 101.6 and 152.4 mm/hr. D ranged from .08 to 10.5 mm and the integration increment, dD , was .08 mm. The results were then approximated by power law equations of the form

$$\alpha_t = a_{RD} R^{b_{RD}} \quad \text{dB/km} \quad , \quad (7)$$

$$Z_{eq} = a_Z R^{b_Z} \quad \text{mm}^6/\text{m}^3 \quad (8)$$

using logarithmic regression analysis to obtain values of a_{RD} , b_{RD} , a_Z and b_Z .

III. RESULTS

Figures 1 and 2 show the equivalent reflectivity, Z_{eq} , and the specific attenuation, α_t , as functions of rain rate for several frequencies. The calculated values (represented by crosses) and the power law regression lines are shown. Clearly, the deviation from the power law is quite small, justifying its use under the assumptions made in these calculations.

The values of a_{RD} , a_Z and b_{RD} , b_Z are shown as functions of frequency in Figures 3 and 4 and Table 1. They are seen to be smoothly varying functions of frequency.

Tables 2 and 3 give the calculated values of the equivalent reflectivity as a function of frequency and rain rate in mm^6/m^3 and dBZ, respectively. The specific attenuation (dB/km) is similarly tabulated in Table 4. Table 5 shows the volumetric radar backscatter cross section in m^2/m^3 , also as a function of frequency and rain rate.

Calculations were also performed from 500 to 1000 GHz. However, at the higher frequencies the reflectivity appeared to be quite sensitive to the method of numerical integration. This appears to be a result of the fact that the incremental drop size, dD , of 0.08 mm could be too coarse since it represents a significant fraction of the wavelength of 0.3 mm at 1000 GHz. Smaller incremental drop sizes caused other computational difficulties; hence, these results were considered to be unreliable and were not included in this report. The specific attenuation did not exhibit the sensitivity described above for the reflectivity.

ZEQ VS. RAIN-RATE

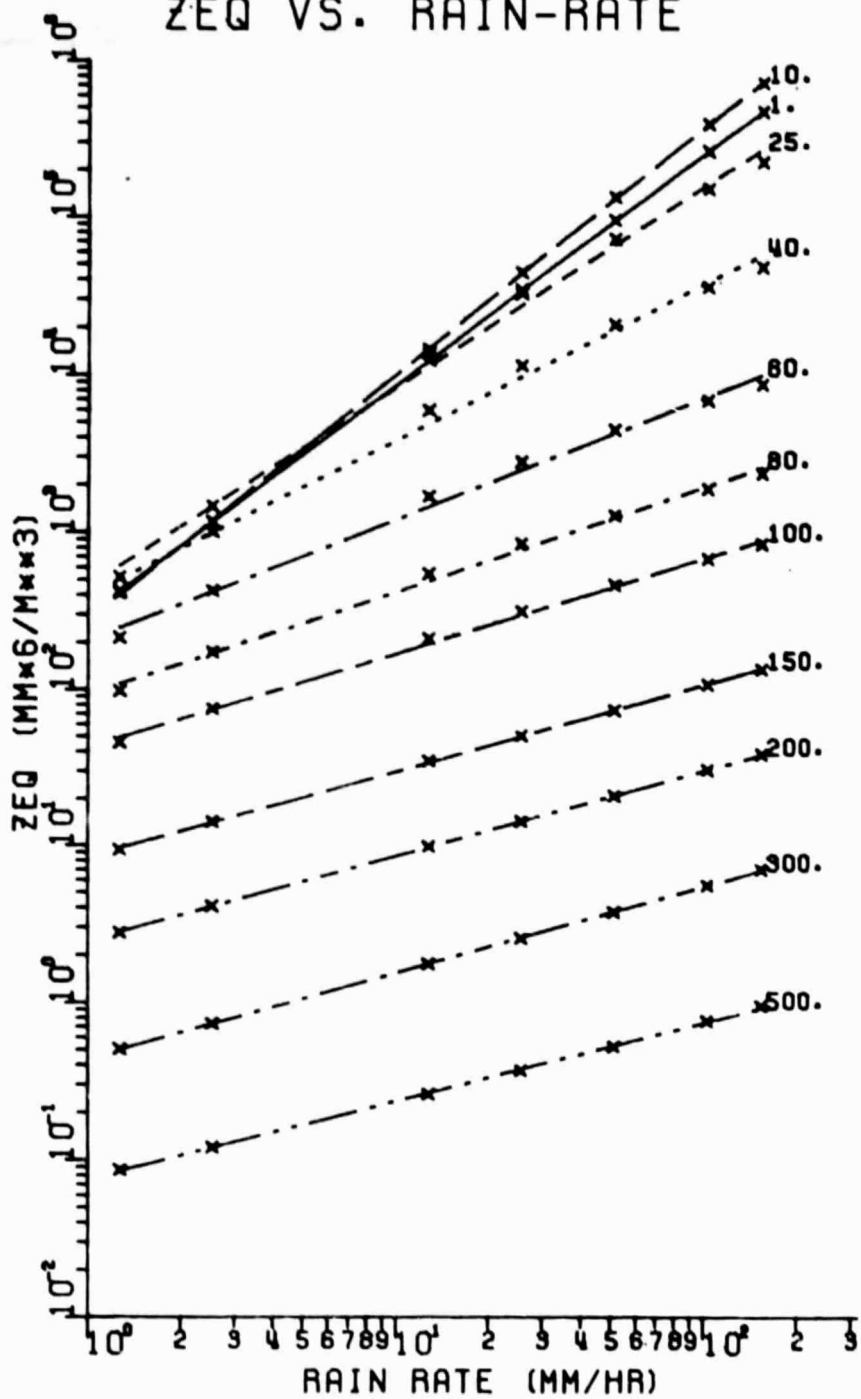


Figure 1. Equivalent reflectivity, Z_{eq} , vs. rain rate at several frequencies.

ATTN. VS. RAIN-RATE

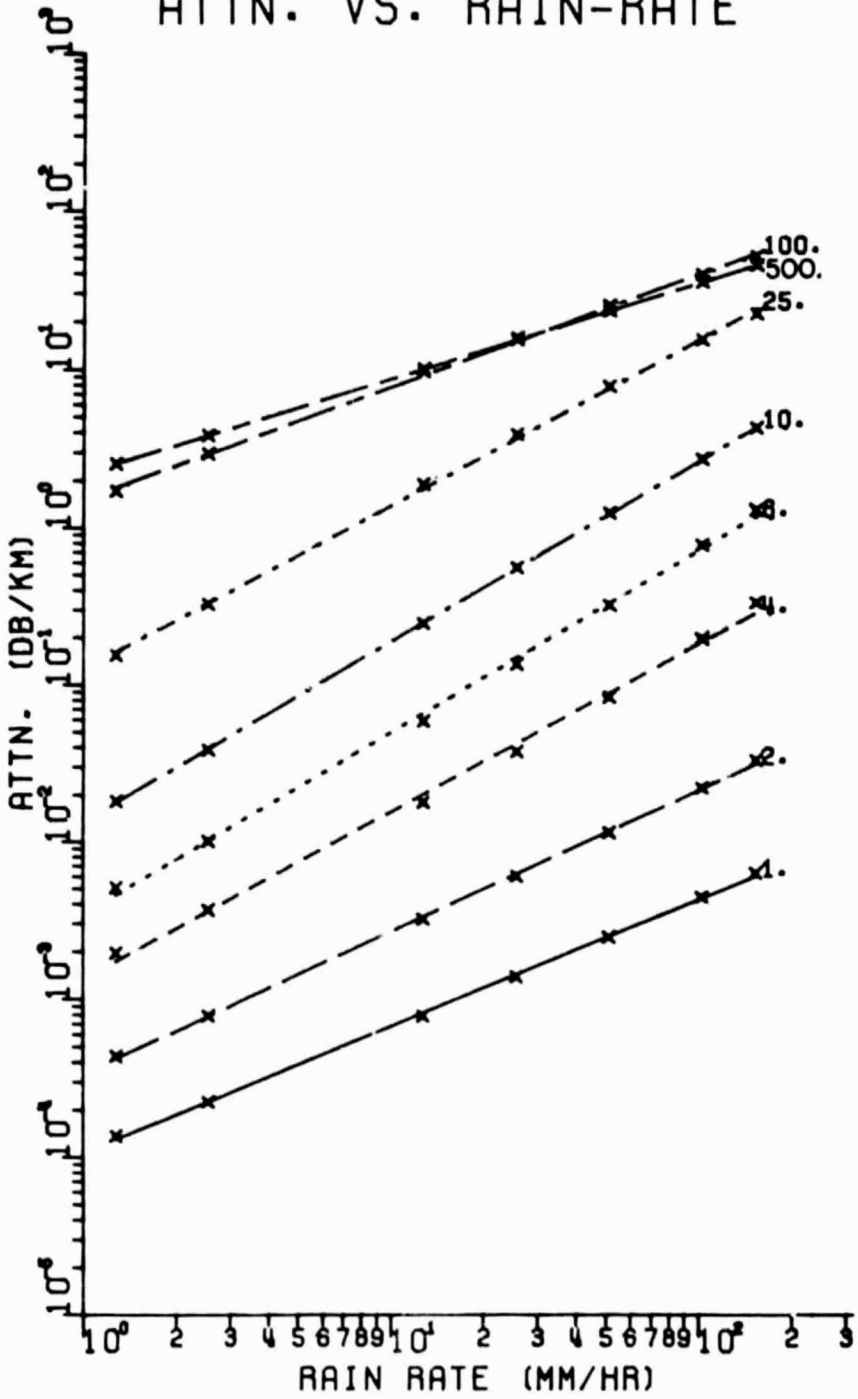


Figure 2. Specific attenuation, α_t , vs. rain rate at several frequencies.

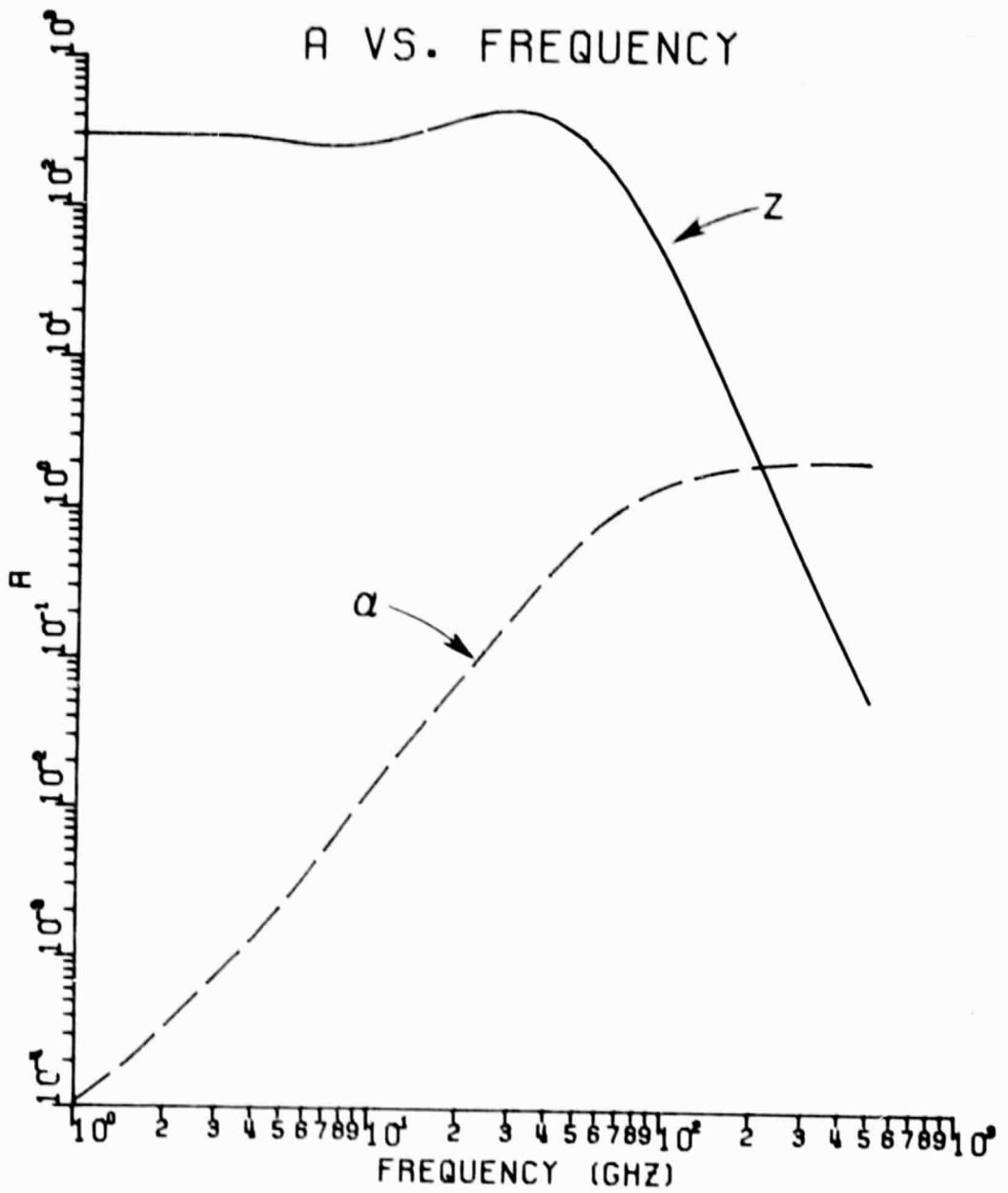


Figure 3. a_z and a_{RD} vs. frequency.

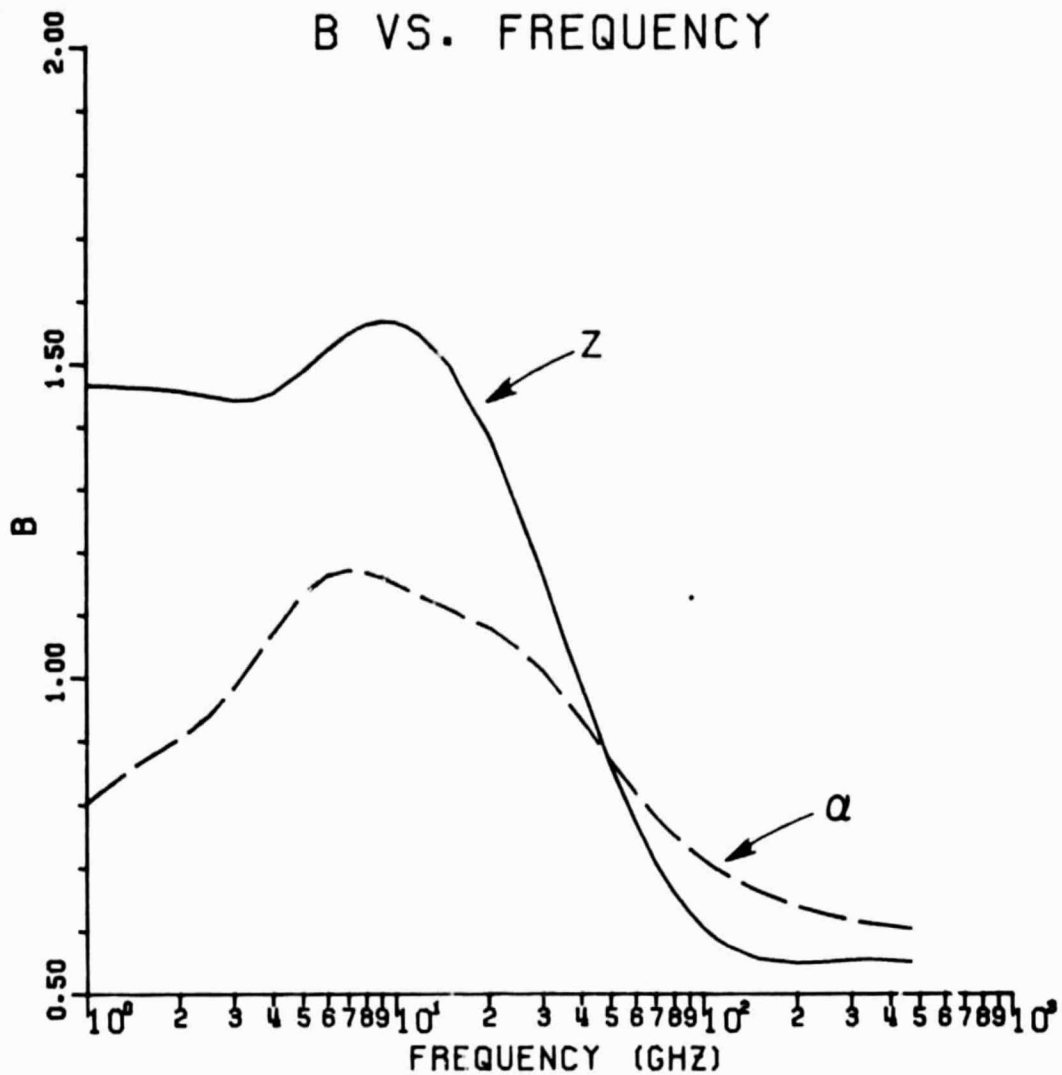


Figure 4. b_Z and b_{RD} vs. frequency.

Table 1
POWER LAW COEFFICIENTS

FREQ. (GHZ)	ZEO		ALPHA	
	A	B	A	B
1.0	2.9622E	2	1.0705E -4	.805
1.5	2.9629E	2	1.9762E -4	.868
2.0	2.9660E	2	3.3694E -4	.904
2.5	2.9724E	2	5.2467E -4	.941
3.0	2.9717E	2	7.5150E -4	.963
3.5	2.9338E	2	1.0211E -3	1.029
4.0	2.8648E	2	1.3446E -3	1.071
5.0	2.7069E	2	2.2139E -3	1.132
6.0	2.6022E	2	3.4753E -3	1.163
7.0	2.5693E	2	5.2129E -3	1.172
8.0	2.5938E	2	7.4711E -3	1.169
9.0	2.6599E	2	1.0261E -2	1.160
10.0	2.7555E	2	1.3572E -2	1.150
11.0	2.8715E	2	1.7382E -2	1.139
12.0	3.0014E	2	2.1673E -2	1.130
15.0	3.4293E	2	3.7351E -2	1.108
20.0	4.0965E	2	7.3659E -2	1.080
25.0	4.5139E	2	1.2545E -1	1.048
30.0	4.5969E	2	1.9496E -1	1.010
35.0	4.3847E	2	2.8178E -1	.972
40.0	3.9775E	2	3.8292E -1	.934
50.0	2.9625E	2	6.0998E -1	.869
60.0	2.0507E	2	8.4106E -1	.819
70.0	1.3789E	2	1.0532E 0	.781
80.0	9.2273E	1	1.2371E 0	.752
90.0	6.2254E	1	1.3318E 0	.730
100.0	4.2625E	1	1.5203E 0	.713
110.0	2.9707E	1	1.6267E 0	.699
120.0	2.1095E	1	1.7152E 0	.687
150.0	8.4153E	0	1.9048E 0	.663
200.0	2.4548E	0	2.0792E 0	.639
250.0	9.3843E	-1	2.1673E 0	.625
300.0	4.3252E	-1	2.2094E 0	.617
350.0	2.2732E	-1	2.2246E 0	.611
400.0	1.3512E	-1	2.2223E 0	.608
500.0	5.4676E	-2	2.1966E 0	.605

Table 2

EQUIVALENT REFLECTIVITY, ZEQ (MM**6/M**3)

FRFQ. (GHZ)	RAIN RATE (MM/HR)													
	1.27	2.54	12.70	25.40	50.80	101.60	152.40							
1.0	4.19E	2	1.16E	3	1.23E	4	3.41E	4	9.42E	4	2.59E	5	4.68E	5
1.5	4.18E	2	1.16E	3	1.23E	4	3.38E	4	9.31E	4	2.55E	5	4.58E	5
2.0	4.17E	2	1.15E	3	1.21E	4	3.34E	4	9.14E	4	2.49E	5	4.45E	5
2.5	4.15E	2	1.15E	3	1.20E	4	3.28E	4	8.92E	4	2.40E	5	4.26E	5
3.0	4.13E	2	1.14E	3	1.18E	4	3.21E	4	8.67E	4	2.32E	5	4.10E	5
3.5	4.11E	2	1.13E	3	1.16E	4	3.15E	4	8.49E	4	2.30E	5	4.15E	5
4.0	4.09E	2	1.12E	3	1.15E	4	3.10E	4	8.46E	4	2.37E	5	4.40E	5
5.0	4.04E	2	1.10E	3	1.13E	4	3.13E	4	8.96E	4	2.68E	5	5.18E	5
6.0	4.00E	2	1.09E	3	1.15E	4	3.32E	4	9.94E	4	3.08E	5	5.97E	5
7.0	3.98E	2	1.09E	3	1.21E	4	3.60E	4	1.10E	5	3.42E	5	6.58E	5
8.0	3.99E	2	1.11E	3	1.24E	4	3.91E	4	1.20E	5	3.67E	5	6.96E	5
9.0	4.02E	2	1.13E	3	1.37E	4	4.19E	4	1.28E	5	3.82E	5	7.14E	5
10.0	4.09E	2	1.16E	3	1.45E	4	4.42E	4	1.35E	5	3.89E	5	7.15E	5
11.0	4.17E	2	1.20E	3	1.52E	4	4.60E	4	1.36E	5	3.88E	5	7.02E	5
12.0	4.26E	2	1.24E	3	1.58E	4	4.72E	4	1.37E	5	3.81E	5	6.78E	5
15.0	4.57E	2	1.35E	3	1.68E	4	4.79E	4	1.30E	5	3.37E	5	5.70E	5
20.0	5.01E	2	1.47E	3	1.61E	4	4.19E	4	1.03E	5	2.35E	5	3.70E	5
25.0	5.20E	2	1.47E	3	1.37E	4	3.25E	4	7.21E	4	1.50E	5	2.23E	5
30.0	5.08E	2	1.36E	3	1.08E	4	2.36E	4	4.82E	4	9.24E	4	1.32E	5
35.0	4.72E	2	1.20E	3	8.10E	3	1.65E	4	3.16E	4	5.70E	4	7.84E	4
40.0	4.21E	2	1.01E	3	5.95E	3	1.15E	4	2.08E	4	3.56E	4	4.78E	4
50.0	3.10E	2	6.71E	2	3.15E	3	5.55E	3	9.24E	3	1.49E	4	1.93E	4
60.0	2.14E	2	4.26E	2	1.64E	3	2.81E	3	4.46E	3	6.87E	3	6.72E	3
70.0	1.45E	2	2.71E	2	9.44E	2	1.50E	3	2.31E	3	3.46E	3	4.35E	3
80.0	9.77E	1	1.74E	2	5.50E	2	8.50E	2	1.28E	3	1.69E	3	2.36E	3
90.0	6.65E	1	1.14E	2	3.35E	2	5.07E	2	7.53E	2	1.10E	3	1.37E	3
100.0	4.60E	1	7.60E	1	2.13E	2	3.17E	2	4.67E	2	6.79E	2	8.44E	2
110.0	3.23E	1	5.21E	1	1.40E	2	2.07E	2	3.03E	2	4.39E	2	5.46E	2
120.0	2.31E	1	3.65E	1	9.53E	1	1.40E	2	2.04E	2	2.96E	2	3.67E	2
150.0	9.38E	0	1.43E	1	3.53E	1	5.14E	1	7.47E	1	1.09E	2	1.35E	2
200.0	2.78E	0	4.12E	0	9.93E	0	1.45E	1	2.11E	1	3.09E	1	3.88E	1
250.0	1.07E	0	1.58E	0	3.78E	0	5.53E	0	8.12E	0	1.20E	1	1.51E	1
300.0	4.98E	-1	7.27E	-1	1.75E	0	2.56E	0	3.78E	0	5.61E	0	7.09E	0
350.0	2.63E	-1	3.83E	-1	9.19E	-1	1.35E	0	2.00E	0	2.97E	0	3.76E	0
400.0	1.54E	-1	2.24E	-1	5.35E	-1	7.83E	-1	1.16E	0	1.73E	0	2.19E	0
500.0	6.36E	-2	9.15E	-2	2.16E	-1	3.17E	-1	4.69E	-1	7.00E	-1	6.89E	-1

Table 3
EQUIVALENT REFLECTIVITY, ZEQ (DBZ)

FREQ. (GHz)	RAIN RATE (MM/HR)					152.40
	1.27	2.54	12.70	25.40	50.80	
1.0	26.2	30.6	40.9	45.3	49.7	54.1
1.5	26.2	30.6	40.9	45.3	49.7	54.1
2.0	26.2	30.6	40.8	45.2	49.6	54.0
2.5	26.2	30.6	40.8	45.2	49.5	53.8
3.0	26.2	30.6	40.7	45.1	49.4	53.7
3.5	26.1	30.5	40.7	45.0	49.3	53.6
4.0	26.1	30.5	40.6	44.9	49.3	53.7
5.0	25.1	30.4	40.5	45.0	49.5	54.5
6.0	26.0	30.4	40.6	45.2	50.0	54.9
7.0	26.0	30.4	40.8	45.6	50.4	55.5
8.0	26.0	30.4	41.1	45.9	50.8	56.4
9.0	26.0	30.5	41.4	46.2	51.1	56.5
10.0	26.1	30.7	41.6	46.5	51.2	56.5
11.0	26.2	30.8	41.8	46.6	51.3	56.5
12.0	26.3	30.9	42.0	46.7	51.4	56.3
15.0	26.6	31.3	42.3	46.8	51.2	57.6
20.0	27.0	31.7	42.1	46.2	50.1	55.7
25.0	27.2	31.7	41.4	45.1	46.6	53.5
30.0	27.1	31.3	40.3	43.7	46.8	51.2
35.0	26.7	30.8	39.1	42.2	45.0	48.9
40.0	26.2	30.0	37.7	40.6	43.2	46.8
50.0	24.9	28.3	35.0	37.4	39.7	42.9
60.0	23.3	26.3	32.3	34.5	36.5	39.4
70.0	21.6	24.3	29.8	31.8	33.6	36.4
80.0	19.9	22.4	27.4	29.3	31.1	33.7
90.0	18.2	20.6	25.3	27.1	28.8	31.4
100.0	16.6	18.8	23.3	25.0	26.7	29.3
110.0	15.1	17.2	21.5	23.2	24.8	27.4
120.0	13.6	15.6	19.8	21.5	23.1	25.7
150.0	9.7	11.5	15.5	17.1	18.7	21.3
200.0	4.4	6.1	10.0	11.6	13.2	15.9
250.0	3	2.0	5.8	7.4	9.1	11.8
300.0	-3.0	-1.4	2.4	4.1	5.2	8.5
350.0	-5.8	-4.2	-0.4	1.3	3.0	5.2
400.0	-8.1	-6.5	-2.7	-1.1	0.6	3.4
500.0	-12.0	-10.4	-6.6	-5.0	-3.3	-1.5

REPRODUCIBILITY OF THE ORIGINAL PAGE IS POOR

Table 5
 VOLUMETRIC RADAR CROSS-SECTION, ETA (M²/M³)

FRFV. (GHz)	RAIN RATE (MM/HR)						152.40
	1.27	2.54	12.70	25.40	50.80	101.60	
1.0	1.48E-11	4.10E-11	4.35E-10	1.20E-9	3.34E-9	9.16E-9	1.65E-8
1.5	7.48E-11	2.07E-10	2.19E-9	6.04E-9	1.66E-8	4.56E-8	8.19E-8
2.0	2.54E-10	6.50E-10	6.85E-9	1.83E-8	5.14E-8	1.40E-7	2.51E-7
2.5	5.72E-10	1.58E-9	1.63E-8	4.52E-8	1.25E-7	3.31E-7	5.87E-7
3.0	1.10E-9	3.25E-9	3.38E-8	9.18E-8	2.48E-7	6.63E-7	1.17E-6
3.5	2.18E-9	5.98E-9	6.16E-8	1.67E-7	4.50E-7	1.22E-6	2.20E-6
4.0	3.69E-9	1.01E-8	1.03E-7	2.80E-7	7.64E-7	2.14E-6	3.97E-6
5.0	8.89E-9	2.43E-8	2.49E-7	6.69E-7	1.97E-6	5.91E-6	1.14E-5
6.0	1.63E-8	4.92E-8	5.26E-7	1.51E-6	4.54E-6	1.40E-5	2.73E-5
7.0	3.56E-8	9.23E-8	1.02E-6	3.04E-6	9.34E-6	2.89E-5	5.56E-5
8.0	5.75E-8	1.59E-7	1.68E-6	5.63E-6	1.73E-5	5.29E-5	1.00E-4
9.0	9.28E-8	2.61E-7	3.17E-6	9.65E-6	2.95E-5	8.82E-5	1.65E-4
10.0	1.44E-7	4.08E-7	5.10E-6	1.55E-5	4.67E-5	1.57E-4	2.51E-4
11.0	2.14E-7	6.17E-7	7.83E-6	2.36E-5	6.98E-5	1.99E-4	3.61E-4
12.0	3.10E-7	9.01E-7	1.15E-5	3.43E-5	9.95E-5	2.77E-4	4.93E-4
15.0	8.09E-7	2.39E-6	2.97E-5	8.46E-5	2.31E-4	5.95E-4	1.01E-3
20.0	2.78E-6	8.14E-6	9.94E-5	2.32E-4	5.88E-4	1.50E-3	2.05E-3
25.0	6.96E-6	1.96E-5	1.83E-4	4.35E-4	9.66E-4	2.01E-3	2.98E-3
30.0	1.39E-5	3.73E-5	2.95E-4	6.46E-4	1.32E-3	2.54E-3	3.61E-3
35.0	2.37E-5	5.99E-5	4.08E-4	8.28E-4	1.58E-3	2.86E-3	3.93E-3
40.0	3.55E-5	8.49E-5	5.01E-4	9.64E-4	1.75E-3	3.00E-3	4.02E-3
50.0	6.14E-5	1.33E-4	6.24E-4	1.10E-3	1.84E-3	2.95E-3	3.83E-3
60.0	8.46E-5	1.69E-4	6.68E-4	1.11E-3	1.76E-3	2.71E-3	3.44E-3
70.0	1.01E-4	1.90E-4	6.62E-4	1.05E-3	1.62E-3	2.43E-3	3.05E-3
80.0	1.12E-4	1.99E-4	6.29E-4	9.71E-4	1.46E-3	2.16E-3	2.69E-3
90.0	1.16E-4	1.99E-4	5.87E-4	8.88E-4	1.32E-3	1.93E-3	2.40E-3
100.0	1.17E-4	1.94E-4	5.42E-4	8.10E-4	1.19E-3	1.73E-3	2.15E-3
110.0	1.15E-4	1.86E-4	5.00E-4	7.40E-4	1.08E-3	1.57E-3	1.95E-3
120.0	1.12E-4	1.77E-4	4.62E-4	6.79E-4	9.89E-4	1.43E-3	1.78E-3
150.0	9.91E-5	1.51E-4	3.75E-4	5.43F-4	7.89E-4	1.15E-3	1.43E-3
200.0	8.02E-5	1.19E-4	2.86E-4	4.16F-4	6.08E-4	8.91E-4	1.12E-3
250.0	5.82E-5	1.00E-4	2.40E-4	3.51E-4	5.15E-4	7.61E-4	9.59E-4
300.0	6.10E-5	8.92E-5	2.14E-4	3.14E-4	4.63E-4	6.27E-4	8.69E-4
350.0	5.66E-5	8.27E-5	1.99E-4	2.92E-4	4.31E-4	6.42E-4	8.13E-4
400.0	5.49E-5	7.96E-5	1.90E-4	2.79E-4	4.12E-4	6.14E-4	7.79E-4
500.0	5.28E-5	7.59E-5	1.79E-4	2.63E-4	3.89E-4	5.61E-4	7.37E-4

IV. SUMMARY

The equivalent reflectivity, Z_{eq} , the specific attenuation, α_t , and the volumetric radar backscatter cross section, η , associated with rain rates from 1.27 to 152.4 mm/hr were calculated for 36 frequencies from 1 to 500 GHz. The rain drops were considered to be dielectric spheres and classical Mie theory was used. No corrections for distortion of the drops were made. The Marshall and Palmer drop size distribution was assumed and the rain temperature was taken to be 0°C.

The results for Z_{eq} , and α_t were then shown to be closely approximated by power laws of the form aR^b over the entire frequency and rain rate ranges considered. The values of the a's and b's were given and shown to be smoothly varying, well behaved functions of frequency.

APPENDIX

SCATTERING BY A DIELECTRIC SPHERE

Consider a dielectric sphere having a radius a and complex relative dielectric constant

$$\epsilon_r = \frac{\epsilon}{\epsilon_0} - j \frac{\sigma}{\omega \epsilon_0} \quad (A1)$$

where,

ϵ_r = relative complex dielectric constant

ϵ = real part of ϵ_r

ϵ_0 = dielectric constant of free space

σ = electrical conductivity of the dielectric

ω = radian frequency.

The complex index of refraction is

$$n_c = \sqrt{\epsilon_r} \quad (A2)$$

Let a plane wave

$$\vec{E}^i = E_0 e^{jkz} \hat{a}_x \quad (A3)$$

be incident on this sphere.

\vec{E}^i = incident electric field of wavelength λ

$k = \frac{2\pi}{\lambda}$ = propagation constant in free space.

Then the attenuation cross section, Q_t , is [4]

$$Q_t = \frac{2\pi}{k^2} \operatorname{Re} \left[\sum_{n=1}^{\infty} (2n+1)(a_n + b_n) \right] \quad m^2, \quad (A4)$$

and the back scatter cross section, Q_b , is

$$Q_b = \frac{\pi}{k^2} \left| \sum_{n=1}^{\infty} (-1)^n (2n+1) (a_n - b_n) \right|^2 m^2 \quad (A5)$$

where the Mie coefficients a_n and b_n are given by

$$a_n = \frac{j_n(n_c \rho) [\rho j_n(\rho)]' - j_n(\rho) [n_c \rho j_n(n_c \rho)]'}{h_n^{(2)}(\rho) [n_c \rho j_n(n_c \rho)]' - j_n(n_c \rho) [\rho h_n^{(2)}(\rho)]'} \quad (A6)$$

$$b_n = \frac{j_n(\rho) [n_c \rho j_n(n_c \rho)]' - n_c^2 j_n(n_c \rho) [\rho j_n(\rho)]'}{n_c^2 j_n(n_c \rho) [\rho h_n^{(2)}(\rho)]' - h_n^{(2)}(\rho) [n_c \rho j_n(n_c \rho)]'} \quad (A7)$$

h_n , j_n and N_n are spherical Hankel and Bessel and Neumann functions, respectively, where

$$\rho = ka \quad (A8)$$

$$h_n^{(2)}(\rho) = j_n(\rho) - j N_n(\rho) \quad (A9)$$

Letting $Z_n = j_n$ or h_n and using the recursion relationships [7]

$$\frac{d}{d\rho} Z_n(\rho) = \frac{1}{2n+1} [nZ_{n-1} - (n+1)Z_{n+1}] \quad (A10)$$

and

$$\begin{aligned} \frac{d[\rho Z_n(\rho)]}{d\rho} &= \rho Z_n'(\rho) + Z_n(\rho) = Z_n(\rho) + \frac{n}{2n+1} \rho Z_{n-1}(\rho), \\ &\quad - \frac{n+1}{2n+1} \rho Z_{n+1}(\rho) \end{aligned} \quad (A11)$$

the derivatives can be eliminated from Equations (A6) and (A7). For $n \geq 1$ a_n and b_n can be rewritten in the form

$$\begin{aligned}
 a_n = & \left\{ j_n(n_c \rho) [nj_{n-1}(\rho) - (n+1)j_{n+1}(\rho)] \right. \\
 & \left. - n_c j_n(\rho) [nj_{n-1}(n_c \rho) - (n+1)j_{n+1}(n_c \rho)] \right\} / \\
 & \left\{ n_c h_n^{(2)}(\rho) [nj_{n-1}(n_c \rho) - (n+1)j_{n+1}(n_c \rho)] \right. \\
 & \left. - j_n(n_c \rho) [nh_{n-1}^{(2)}(\rho) - (n+1)h_{n+1}^{(2)}(\rho)] \right\} \quad (A12)
 \end{aligned}$$

$$\begin{aligned}
 b_n = & \left\{ j_n(\rho) \left[j_n(n_c \rho) + \frac{n_c \rho}{2n+1} [nj_{n-1}(n_c \rho) - (n+1)j_{n+1}(n_c \rho)] \right] \right. \\
 & \left. - n_c j_n(n_c \rho) \left[n_c j_n(\rho) + \frac{n_c \rho}{2n+1} [nj_{n-1}(\rho) - (n+1)j_{n+1}(\rho)] \right] \right\} / \\
 & \left\{ n_c j_n(n_c \rho) \left[n_c h_n^{(2)}(\rho) + \frac{n_c \rho}{2n+1} [nh_{n-1}^{(2)}(\rho) - (n+1)h_{n+1}^{(2)}(\rho)] \right] \right. \\
 & \left. - h_n^{(2)}(\rho) \left[j_n(n_c \rho) + \frac{n_c \rho}{2n+1} [nj_{n-1}(n_c \rho) - (n+1)j_{n+1}(n_c \rho)] \right] \right\} \quad (A13)
 \end{aligned}$$

which is more suitable for computational purposes. Similarly, for $n=0$:

$$\begin{aligned}
 a_0 = & \left\{ n_c j_0(\rho) j_1(n_c \rho) - j_0(n_c \rho) j_1(\rho) \right\} / \\
 & \left\{ j_0(n_c \rho) h_1^{(2)}(\rho) - n_c h_0^{(2)}(\rho) j_1(n_c \rho) \right\} \quad (A14)
 \end{aligned}$$

$$\begin{aligned}
b_0 = & \left\{ j_0(\rho) [j_0(n_c \rho) - n_c \rho j_1(n_c \rho)] \right. \\
& \left. - n_c j_0(n_c \rho) [n_c j_0(\rho) - n_c \rho j_1(\rho)] \right\} / \\
& \left\{ n_c j_0(n_c \rho) [n_c h_0^{(2)}(\rho) - n_c \rho h_1^{(2)}(\rho)] \right. \\
& \left. - h_0^{(2)}(\rho) [j_0(n_c \rho) - n_c \rho j_1(n_c \rho)] \right\} .
\end{aligned} \tag{A15}$$

REFERENCES

- [1] D. B. Hodge, "Meteorological Radar Calibration," Report 784650-1, (in preparation), The Ohio State University ElectroScience Laboratory, Department of Electrical Engineering; prepared under Contract NAS5-23850 for National Aeronautics and Space Administration.
- [2] R. L. Olsen, D. V. Rogers and D. B. Hodge, "The aR^b Relation in the Calculation of Rain Attenuation," Accepted for publication in IEEE Transactions on Antennas and Propagation.
- [3] L. J. Battan, "Radar Observations of the Atmosphere," The University of Chicago Press, 1973, pp. 88-97.
- [4] D. E. Kerr, ed., Propagation of Short Radio Waves, Dover Publications Inc., 1965, pp. 445-454.
- [5] D. B. Hodge, "The Effects of Precipitation on Radar Target Identification and Imaging," Report 2374-19, November 1975, The Ohio State University ElectroScience Laboratory, Department of Electrical Engineering; prepared under Grant No. NGR 36-008-080 for National Aeronautics and Space Administration.
- [6] J. S. Marshall and W. M. K. Palmer, "The Distribution of Raindrops with Size," *J. Meteor.*, Vol. 5, 1948, pp. 165-166.
- [7] J. A. Stratton, Electromagnetic Theory, McGraw-Hill, 1941, p. 406.